Symmetry-protected skyrmions in three-dimensional spin-orbit-coupled Bose gases

Guanjun Chen,[1,2] Tiantian Li,[1] and Yunbo Zhang[1,*]
[1]*Institute of Theoretical Physics, Shanxi University, Taiyuan 030006, China*
[2]*Department of Physics, Taiyuan Normal University, Taiyuan 030001, China*
(Received 2 March 2015; published 26 May 2015)

We present a variational study of pseudo-spin-1/2 Bose gases in a harmonic trap with weak three-dimensional (3D) spin-orbit coupling of $\boldsymbol{\sigma}\cdot\mathbf{p}$ type. This spin-orbit coupling mixes states with different parities, which inspires us to approximate the single-particle state with the eigenstates of the total angular momentum, i.e., superposition of harmonic s-wave and p-wave states. As the time-reversal symmetry is protected by two-body interaction, we set the variational order parameter as the combination of two mutually time-reversal symmetric eigenstates of the total angular momentum. The variational results essentially reproduce the 3D skyrmionlike ground state recently identified by Kawakami *et al.* [T. Kawakami, T. Mizushima, M. Nitta, and K. Machida, Phys. Rev. Lett. **109**, 015301 (2012)]. We show that these skyrmionlike ground states emerging in this model are primarily caused by the p-wave spatial mode involved in the variational order parameter that drives two spin components spatially separated. We find the ground state of this system falls into two phases with different density distribution symmetries depending on the relative magnitude of intraspecies and interspecies interaction: phase I has parity symmetric and axisymmetric density distributions, while phase II is featured with special joint symmetries of discrete rotational and time-reversal symmetry. With the increasing interaction strength the transition occurs between two phases with distinct density distributions, while the topological 3D skyrmionlike spin texture is symmetry protected.

DOI: 10.1103/PhysRevA.91.053624 PACS number(s): 67.85.Fg, 03.75.Mn, 67.85.Jk, 03.75.Lm

I. INTRODUCTION

The experimental realization [1,2] of one-dimensional (1D) spin-orbit (SO) coupling in pseudo-spin-1/2 Bose gases has stimulated many theoretical works on SO coupling in cold atom physics. These works range from Raman induced 1D SO coupling [3–7] that has been realized in cold atoms to more symmetric two-dimensional (2D) Rashba configuration [7–16] that has been extensively studied in condensed matter. In the absence of a harmonic trap, single-particle ground states of both Raman induced and Rashba SO coupling are degenerate, and two-body interaction selects the generic ground state from the degenerate manifold determined by the interaction parameters. For example, Wang *et al.* [8] found that two distinct ground-state phases, namely, the plane-wave and standing-wave (or stripe) phases, appear when intraspecies two-body interaction is larger or smaller than interspecies interaction, respectively, in homogeneous 2D Rashba SO-coupled pseudo-spin-1/2 Bose gases. In the presence of a 2D harmonic trap, a more complex phase diagram of Rashba SO-coupled Bose gases with two classes of phases and several subphases in each was figured out by Hu *et al.* [10,11].

Now experimental schemes for the realization of Rashba SO coupling have been proposed such as in [17]. On the other hand, the most symmetric three-dimensional (3D) SO coupling or Weyl coupling [18–24], which does not even exist in solid matter, is expected to be realizable in cold atom gases, and experimental schemes for that have also been proposed theoretically [18,19]. Recently, Kawakami *et al.* [20] identified a 3D skyrmion ground state in 3D SO-coupled two-component bosons by numerically minimizing the Gross-Pitaevskii energy functional of the system. They explained the stability of 3D skyrmion ground state as a result of helical modulation of the order parameter in the presence of SO coupling. The interaction in their work is supposed to be SU(2) symmetric. Even though two skyrmionlike ground states are found to be stabilized in different interaction regimes, a ground-state phase diagram is still absent now. In another work by Li *et al.* [21], the 3D skyrmionlike ground state is found to emerge in the weak SO-coupling regime, while the skyrmion lattice arises in the strong SO-coupling regime.

In this work, we consider a pseudo-spin-1/2 boson system subject to 3D SO coupling of $\boldsymbol{\sigma}\cdot\mathbf{p}$ type in a harmonic trap, and aim to elucidate the role of interaction in determining the ground-state density and spin texture therein. In Sec. II we introduce the energy functional for the model in rescaled units of length, energy, interaction, and SO-coupling strength. In the weak SO-coupling case, the single-particle energy levels are essentially harmonic oscillatorlike [22], and SO coupling will mix states with different parities while keeping the total angular momentum a conservative. In Sec. III we first try to couple the two lowest s- and p-wave states with the same total angular momentum 1/2 into two spinor wave functions with total angular momentum magnetic quantum number $\pm 1/2$ that are time-reversal states of each other. Then we set the variational order parameter as the superposition of these two states just as has been done in 1D and 2D cases [3,8]. Finally, we calculate the energy functional using the proposed variational order parameter. In Sec. IV the ground-state phase diagram is determined by numerically minimizing the energy functional with respect to the variational parameters; we illustrate the density and spin texture for the two phases. Section V summarizes our main results.

II. MODEL

We consider a pseudo-spin-1/2 boson system confined in a harmonic trap with a weak Weyl type 3D spin-orbit coupling

*ybzhang@sxu.edu.cn

$\boldsymbol{\sigma}\cdot\mathbf{p}$. The system is described by its Gross-Pitaevskii energy functional under the mean-field approximation

$$\mathcal{E}=\mathcal{E}_0+\mathcal{E}_{\rm int}, \tag{1}$$

where the single-particle part is

$$\mathcal{E}_0=\int d^3\mathbf{r}\Psi^\dagger(\mathbf{r})\left(\frac{\mathbf{p}^2}{2m}+\frac{1}{2}m\omega^2r^2+\lambda\boldsymbol{\sigma}\cdot\mathbf{p}\right)\Psi(\mathbf{r}) \tag{2}$$

with m the mass of atoms and ω the trap frequency. $\Psi=(\psi_\uparrow,\psi_\downarrow)^T$ denotes spinor order parameters for bosons with pseudospin states $\uparrow$, $\downarrow$, $\boldsymbol{\sigma}=(\sigma_x,\sigma_y,\sigma_z)$ are the Pauli matrices, and λ parametrizes the SO-coupling strength. The interaction $\mathcal{E}_{\rm int}$ takes the usual contact form of s-wave scattering interaction [25]. We assume now [8,10,11,21] the two intraspecies interaction parameters being the same $g_{\uparrow\uparrow}=g_{\downarrow\downarrow}=g$ and define the relative magnitude of the interspecies and intraspecies parameters as $c=g_{\uparrow\downarrow}/g_{\uparrow\uparrow}$. The interaction part is then

$$\mathcal{E}_{\rm int}=\frac{1}{4}\int d^3\mathbf{r}\big[(g+cg)n^2+4(g-cg)S_z^2\big]. \tag{3}$$

In Eq. (3), $n(\mathbf{r})=n_\uparrow(\mathbf{r})+n_\downarrow(\mathbf{r})$ is the particle density and S_z is the z component of the spin density $\mathbf{S}=\frac{1}{2}\Psi^\dagger\sigma\Psi$ with $n_{\uparrow,\downarrow}(\mathbf{r})=|\psi_{\uparrow,\downarrow}(\mathbf{r})|^2$ the particle densities of two components, respectively. The corresponding Hamiltonian is time-reversal symmetric with the time-reversal operator defined as $T=-i\sigma_yK$ and K denotes the complex conjugate. The system has length scale of the trapping potential $l_T=\sqrt{\hbar/m\omega}$, energy scale $\hbar\omega$, interaction strength scale $\hbar\omega l_T^3/N$, and SO-coupling strength scale $\sqrt{\hbar\omega/m}$. If we further normalize the order parameter to unity, i.e., $\Psi\to\sqrt{N/l_T^3}\Psi$ with N the total particle number in the condensate, the energy functional per particle is obtained as

$$\begin{aligned}\epsilon=&\int d^3\mathbf{r}\Psi^\dagger(\mathbf{r})\left\{-\frac{\nabla^2}{2}+\frac{r^2}{2}+\lambda\boldsymbol{\sigma}\cdot\mathbf{p}\right\}\Psi(\mathbf{r})\\&+\frac{1}{4}\int d^3\mathbf{r}\big((g+cg)n^2+4(g-cg)S_z^2\big).\end{aligned} \tag{4}$$

III. VARIATIONAL APPROACH

In the case of weak SO coupling the single-particle energy spectrum in our system should be harmonic oscillatorlike as proposed in [21,22]. The three-dimensional harmonic oscillator thus proves to be a good choice of the trial wave function, upon which we may develop our variational method. As can be seen later the spin-orbit coupling induces transition between eigenstates with the same total angular momentum but different parity, which are mixed into the variational wave function. The interaction Hamiltonian further couples the two time-reversal states with different weight factors due to the anisotropic interaction parameter ratio c.

A. Variational order parameter

The eigenequation of the three-dimensional harmonic oscillator, $(-\frac{\nabla^2}{2}+\frac{r^2}{2})\phi=\varepsilon\phi$, has well-known solutions, with energy eigenvalues $\varepsilon_{n_rl}=2n_r+l+\frac{3}{2}$ and eigenfunctions $\phi_{n_rlm_l}(r,\theta,\varphi)=R_{n_rl}(r)Y_{lm_l}(\theta,\varphi)$. Here n_r is the radial quantum number, l is the orbital angular momentum quantum number with m_l its magnetic quantum number, R_{n_rl} is the radial wave function, and Y_{lm_l} is the spherical harmonics. The Casimir operator $\mathbf{l}^2$ and $\mathbf{s}^2$ for the orbital and spin angular momenta and their z components are all conservatives in the harmonic oscillator problem. In order to take into account the spin-orbital-coupling term $\boldsymbol{\sigma}\cdot\mathbf{p}$, it is convenient to choose the coupled representation of angular momentum, i.e., the complete set of commutative operators $\mathbf{l}^2,\mathbf{s}^2,\mathbf{j}^2,j_z$ where $\mathbf{j}=\mathbf{l}+\mathbf{s}$ and j_z denote the total angular momentum and its z component, respectively. The eigenfunction $\phi_{n_rlm_l}(r,\theta,\varphi)$ should be combined with the spin wave function χ_{m_s} in the coupled representation as

$$\phi_{n_rljm_j}(r,\theta,\varphi)=R_{n_rl}(r)Y^l_{jm_j}(\Omega), \tag{5}$$

where $Y^l_{jm_j}(\Omega)=\sum_{m_l,m_s}C^{jm_j}_{lm_l\frac{1}{2}m_s}Y_{lm_l}\chi_{m_s}$ is the spinor spherical harmonics [26] with $j=l\pm1/2$ and $C^{jm_j}_{lm_l\frac{1}{2}m_s}$ the Clebsch-Gordan coefficients. In the coupled representation, the ground-state wave function has $n_r=l=0$. This gives a total angular momentum $j=\frac{1}{2}$ with $m_j=\pm\frac{1}{2}$ and the two degenerate ground states are

$$\phi_{00\frac{1}{2}\pm\frac{1}{2}}(\mathbf{r})=R_{00}(r)Y^0_{\frac{1}{2}\pm\frac{1}{2}}(\Omega), \tag{6}$$

respectively. Because the SO-coupling term breaks the parity symmetry, it can couple s- and p-wave states with the same total angular momentum $\mathbf{j}$ and j_z [21]. Keeping these considerations in mind, in the simplest approximation, we suppose the ground state contains only the lowest s- and p-wave states with total angular momentum quantum number $j=\frac{1}{2}$ in the presence of the SO-coupling term. The state with $m_j=\frac{1}{2}$ takes the form

$$\Phi_{j=\frac{1}{2},m_j=\frac{1}{2}}=N_\alpha\big(\phi_{00\frac{1}{2}\frac{1}{2}}+i\alpha\phi_{01\frac{1}{2}\frac{1}{2}}\big) \tag{7}$$

where $N_\alpha=(1+\alpha^2)^{-1/2}$, α stands for the relative weight of the s and p orbital modes, and i in front of α originates from the pure imaginary matrix element of the SO coupling between the two states in Eq. (7). This hypothesis is similar to that appearing in [21] and [22], and has been verified numerically [21]. Explicitly this state is a spinor:

$$\Phi_{j=\frac{1}{2},m_j=\frac{1}{2}}=N_\alpha\begin{pmatrix}R_{00}Y_{00}-i\alpha\sqrt{\frac{1}{3}}R_{01}Y_{10}\\ i\alpha\sqrt{\frac{2}{3}}R_{01}Y_{11}\end{pmatrix}. \tag{8}$$

The state with $m_j=-\frac{1}{2}$ takes the form

$$\Phi_{j=\frac{1}{2},m_j=-\frac{1}{2}}=N_\alpha\big(\phi_{00\frac{1}{2}-\frac{1}{2}}+i\alpha\phi_{01\frac{1}{2}-\frac{1}{2}}\big) \tag{9}$$

and similarly we have

$$\Phi_{j=\frac{1}{2},m_j=-\frac{1}{2}}=N_\alpha\begin{pmatrix}-i\alpha\sqrt{\frac{2}{3}}R_{01}Y_{1-1}\\ R_{00}Y_{00}+i\alpha\sqrt{\frac{1}{3}}R_{01}Y_{10}\end{pmatrix} \tag{10}$$

which is nothing but the time reversal of $\Phi_{j=\frac{1}{2},m_j=\frac{1}{2}}$. In the single-particle level, $\Phi_{j=\frac{1}{2},m_j=\pm\frac{1}{2}}$ and any normalized superposition of them having the same energy thus are "degenerate"

single-particle states, which is similar to degeneracy indicated by the Kramers theorem in the spin-1/2 system.

The single-particle states exhibit infinite-fold degeneracy and we expect this degeneracy can be partially resolved by the interaction which would pick up the ground state from these degenerate states as in the case of Rashba spin-orbital coupling considered by Wang *et al.* [8]. Since the interaction does not break the time-reversal symmetry, the residual twofold Kramers degeneracy needs to be considered in the wave function [2]. We therefore set the variational order parameter as

$$\Psi = c_+\Phi + c_- T\Phi = \begin{pmatrix} c_+\Phi_\uparrow - c_-\Phi_\downarrow^* \\ c_+\Phi_\downarrow + c_-\Phi_\uparrow^* \end{pmatrix}, \tag{11}$$

with the constraint $c_+^2 + c_-^2 = 1$. Here $\Phi \equiv \Phi_{j=\frac{1}{2},m_j=\frac{1}{2}}$ and $\Phi_{\uparrow,\downarrow}$ are its up and down components. So far, we have introduced three variational parameters α, c_+, c_- and the energy functional of Eq. (4) can be calculated analytically using the proposed order parameter (11).

B. Energy functional

We calculate the energy functional on the variational wave function (11). The contribution comes from two parts, the single particle and the interaction Hamiltonian. We notice that for the kinetic and trapping potential terms the nonzero integral contribution comes from those states with the same parities, while the spin-orbital-coupling $\boldsymbol{\sigma}\cdot\mathbf{p}$ term will mix states with opposite parities, i.e.,

$$\begin{aligned}\int d^3\mathbf{r}\Psi^\dagger(\mathbf{r})\Big\{-\frac{\nabla^2}{2}+\frac{r^2}{2}+\lambda\boldsymbol{\sigma}\cdot\mathbf{p}\Big\}\Psi(\mathbf{r}) \\ = N_\alpha^2\Big[\Big\langle\phi_{00\frac{1}{2}\frac{1}{2}}\Big|\Big(-\frac{\nabla^2}{2}+\frac{r^2}{2}\Big)\Big|\phi_{00\frac{1}{2}\frac{1}{2}}\Big\rangle \\ +\alpha^2\Big\langle\phi_{01\frac{1}{2}\frac{1}{2}}\Big|\Big(-\frac{\nabla^2}{2}+\frac{r^2}{2}\Big)\Big|\phi_{01\frac{1}{2}\frac{1}{2}}\Big\rangle \\ +i2\alpha\langle\phi_{00\frac{1}{2}\frac{1}{2}}|\lambda\boldsymbol{\sigma}\cdot\mathbf{p}|\phi_{01\frac{1}{2}\frac{1}{2}}\rangle\Big].\end{aligned} \tag{12}$$

Here we have used

$$\begin{aligned}\langle\phi_{00\frac{1}{2}\frac{1}{2}}|\lambda\boldsymbol{\sigma}\cdot\mathbf{p}|\phi_{01\frac{1}{2}\frac{1}{2}}\rangle \\ = \langle\phi_{00\frac{1}{2}-\frac{1}{2}}|\lambda\boldsymbol{\sigma}\cdot\mathbf{p}|\phi_{01\frac{1}{2}-\frac{1}{2}}\rangle,\end{aligned} \tag{13}$$

which is on account of $[j_z,\boldsymbol{\sigma}\cdot\mathbf{p}]=0$.

It is crucial to calculate the contribution of the spin-orbital-coupling term by means of the irreducible tensor method [26]. To this end we first introduce the irreducible form of the spin-orbital coupling term. The irreducible tensor form of the momentum operator is [26]

$$p^{(1)} = i\sqrt{2}\frac{1}{r}\{C^{(1)}l^{(1)}\}^{(1)} - i\frac{\partial}{\partial r}C^{(1)}, \tag{14}$$

where $C^{(1)}$ and $l^{(1)}$ are rank-1 irreducible tensors of the unit vector $\hat{\mathbf{r}}$ and the orbital angular momentum $\mathbf{l}$, and $\{A^{(m)}B^{(n)}\}^{(k)}$ defines the rank-k tensor product of rank-m irreducible tensor $A^{(m)}$ and rank-n irreducible tensor $B^{(n)}$. According to [26], the dot product of two arbitrary vectors $\mathbf{A}$ and $\mathbf{B}$ is related to the tensor product through $\mathbf{A}\cdot\mathbf{B} = -\sqrt{3}\{A^{(1)}B^{(1)}\}^{(0)}$. In our case, the radial coordinate r can be separated from the spin and spherical parts accordingly,

$$\begin{aligned}\boldsymbol{\sigma}\cdot\mathbf{p} = &-i\frac{\sqrt{6}}{r}\big\{\sigma^{(1)}\{C^{(1)}l^{(1)}\}^{(1)}\big\}^{(0)} \\ &+i\sqrt{3}\frac{\partial}{\partial r}\{\sigma^{(1)}C^{(1)}\}^{(0)},\end{aligned} \tag{15}$$

such that

$$\begin{aligned}&\langle\phi_{00\frac{1}{2}\frac{1}{2}}|\boldsymbol{\sigma}\cdot\mathbf{p}|\phi_{01\frac{1}{2}\frac{1}{2}}\rangle \\ &= -i\sqrt{6}\langle R_{00}(r)|\frac{1}{r}|R_{01}(r)\rangle \\ &\quad\times\big\langle Y^0_{\frac{1}{2}\frac{1}{2}}(\Omega)\big|\big\{\sigma^{(1)}\{C^{(1)}l^{(1)}\}^{(1)}\big\}^{(0)}\big|Y^1_{\frac{1}{2}\frac{1}{2}}(\Omega)\big\rangle \\ &\quad+i\sqrt{3}\langle R_{00}(r)|\frac{d}{dr}|R_{01}(r)\rangle \\ &\quad\times\big\langle Y^0_{\frac{1}{2}\frac{1}{2}}(\Omega)\big|\{\sigma^{(1)}C^{(1)}\}^{(0)}\big|Y^1_{\frac{1}{2}\frac{1}{2}}(\Omega)\big\rangle.\end{aligned} \tag{16}$$

The integrals for the radial coordinates are easy to calculate:

$$\langle R_{00}(r)|\frac{1}{r}|R_{01}(r)\rangle = \sqrt{\frac{2}{3}}, \tag{17}$$

$$\langle R_{00}(r)|\frac{d}{dr}|R_{01}(r)\rangle = -\frac{1}{\sqrt{6}}, \tag{18}$$

where $R_{00}(r) = \sqrt{2^2/\sqrt{\pi}}e^{-r^2/2}$ and $R_{01}(r) = \sqrt{2^3/(3\sqrt{\pi})}re^{-r^2/2}$ are used. The Wigner-Eckart theorem can be used to calculate the angular and spin integrals:

$$\big\langle Y^0_{\frac{1}{2}\frac{1}{2}}(\Omega)\big|\big\{\sigma^{(1)}\{C^{(1)}l^{(1)}\}^{(1)}\big\}^{(0)}\big|Y^1_{\frac{1}{2}\frac{1}{2}}(\Omega)\big\rangle = \frac{1}{\sqrt{6}}, \tag{19}$$

$$\big\langle Y^0_{\frac{1}{2}\frac{1}{2}}(\Omega)\big|\{\sigma^{(1)}C^{(1)}\}^{(0)}\big|Y^1_{\frac{1}{2}\frac{1}{2}}(\Omega)\big\rangle = \frac{1}{\sqrt{3}}. \tag{20}$$

Substituting Eqs. (17)–(20) into Eq. (16), one has

$$\langle\phi_{00\frac{1}{2}\frac{1}{2}}|\boldsymbol{\sigma}\cdot\mathbf{p}|\phi_{01\frac{1}{2}\frac{1}{2}}\rangle = -i\sqrt{\frac{3}{2}}. \tag{21}$$

Hence the single-particle part of the energy functional is

$$\begin{aligned}\int d^3\mathbf{r}\Psi^\dagger(\mathbf{r})\Big\{-\frac{\nabla^2}{2}+\frac{r^2}{2}+\lambda\boldsymbol{\sigma}\cdot\mathbf{p}\Big\}\Psi(\mathbf{r}) \\ = N_\alpha^2\Big(\frac{3}{2}+\frac{5}{2}\alpha^2+\sqrt{6}\alpha\lambda\Big)\end{aligned} \tag{22}$$

where we have used that the eigenenergies of the s and p states of the three-dimensional oscillator are, respectively, $\varepsilon_{00} = 3/2$ and $\varepsilon_{01} = 5/2$.

For the calculation of the interaction part of the energy functional, it is easy to show that the total density n is always spherical symmetric,

$$n = |\Phi|^2 = (4\pi)^{-1}N_\alpha^2\big(R_{00}^2 + \alpha^2R_{01}^2\big), \tag{23}$$

and the density-density interaction energy is

$$\int d^3\mathbf{r}n^2 = \frac{1}{12}N_\alpha^4(2\pi)^{-\frac{3}{2}}(5\alpha^4+12\alpha^2+12). \tag{24}$$

On the other hand, the spin density is anisotropic; e.g., the z component takes the form of

$$S_z = (8\pi)^{-1} N_\alpha^2 \{(c_+^2 - c_-^2)(R_{00}^2 + \alpha^2 R_{01}^2 \cos 2\theta) - (2c_+c_-)(2\alpha R_{00} R_{01} \sin\theta \sin\varphi - \alpha^2 R_{01}^2 \sin 2\theta \cos\varphi)\}, \tag{25}$$

and the spin-spin interaction energy is integrated as

$$\int d^3\mathbf{r} S_z^2 = \frac{1}{4} N_\alpha^4 (2\pi)^{-\frac{3}{2}} \left[\frac{1}{36}(7\alpha^4 - 12\alpha^2 + 36) - \frac{1}{3} c_+^2 c_-^2 (\alpha^4 - 12\alpha^2 + 12)\right]. \tag{26}$$

Collecting Eqs. (22), (24), and (26) into Eq. (4), we finally arrive at the variational result for the ground-state energy per particle:

$$\epsilon = N_\alpha^2 \left(\frac{3}{2} + \frac{5}{2}\alpha^2 + \sqrt{6}\alpha\lambda\right) + N_\alpha^4 (2\pi)^{-\frac{3}{2}} \frac{1}{72} \times [(11\alpha^4 + 12\alpha^2 + 36)g + (4\alpha^4 + 24\alpha^2)cg - 6c_+^2 c_-^2 (g - cg)(\alpha^4 - 12\alpha^2 + 12)]. \tag{27}$$

IV. GROUND-STATE PHASE DIAGRAM

The ground-state phase diagram can be determined numerically via the minimization of the variational energy with respect to the parameters α, c_+, and c_- for given c and g. We notice that the parameters c_+ and c_- appear only in the last term of Eq. (27) in the form of $c_+^2 c_-^2$, the value of which ranges from zero to one-quarter. The parameter $c_+^2 c_-^2$ as a whole takes the value of either zero or one-quarter in the minimization, depending on the signs of $(g - cg)$ and $f(\alpha) = \alpha^4 - 12\alpha^2 + 12$. The ground state thus falls into two classes of phases as depicted in Fig. 1: in phase I, the variation yields $|c_+|^2 = 1$, $|c_-|^2 = 0$, or $|c_+|^2 = 0$, $|c_-|^2 = 1$; in phase II, the variation yields $|c_+|^2 = |c_-|^2 = 1/2$. It is clear that α must be negative for a positive λ due to the fact that α's in Eq. (27) are all even ordered except the spin-orbital-coupling term. We see that $c = 1$ divides the phase plane into upper and lower regions. With increasing g the system enters alternately into phases I and II and the boundaries are determined by $f(\alpha) = 0$, i.e., $\alpha_\pm = -\sqrt{6 \pm 2\sqrt{6}}$. For typical experiments with the ^{87}Rb condensate, the interaction strength scale is $10^{-13}\,\mathrm{Hz\,cm^3}$, which gives rise to $g \sim 40$–80. For smaller g, $\alpha \geqslant \alpha_-$ results in a positive value of $f(\alpha)$ such that the $c > 1$ region belongs to phase I and $c < 1$ belongs to phase II. By adjusting the trapping frequency and the density of the condensate one can easily increase g to cross the critical line such that $\alpha \in [\alpha_+, \alpha_-]$, which makes $f(\alpha)$ negative. We observe an interesting swap of the phases: $c < 1$ corresponds to phase I and $c > 1$ corresponds to phase II. A similar phase transition appears in the Rashba spin-orbital-coupled bosons [10,11]. Further increasing the interaction strength makes the optimized parameter $\alpha \leqslant \alpha_+$ and the phases swap occurs again.

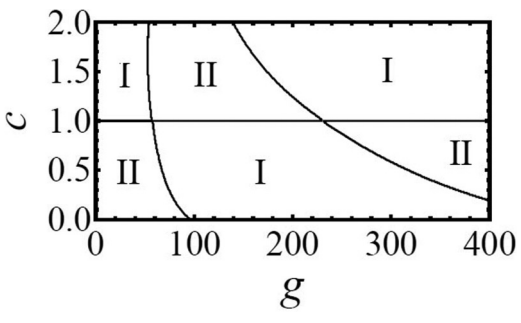

FIG. 1. Phase diagram of weakly SO-coupled two-component bosons with coupling strength $\lambda = 0.2\sqrt{\hbar\omega/m}$, which shows two skyrmionlike phases I and II. Phase I is a skyrmion ground state of order parameter $\exp[-i\Omega(\mathbf{r})\cdot\mathbf{S}]\boldsymbol{\zeta}$ with $\boldsymbol{\zeta}_z = (1,0)^T$ and phase II is a skyrmion state with $\boldsymbol{\zeta}_x = \frac{1}{\sqrt{2}}(1,1)^T$. The interaction parameter g is in units of $\hbar\omega l_T^3/N$. Density distribution and spin texture of these two phases are shown in Figs. 2 and 3, respectively.

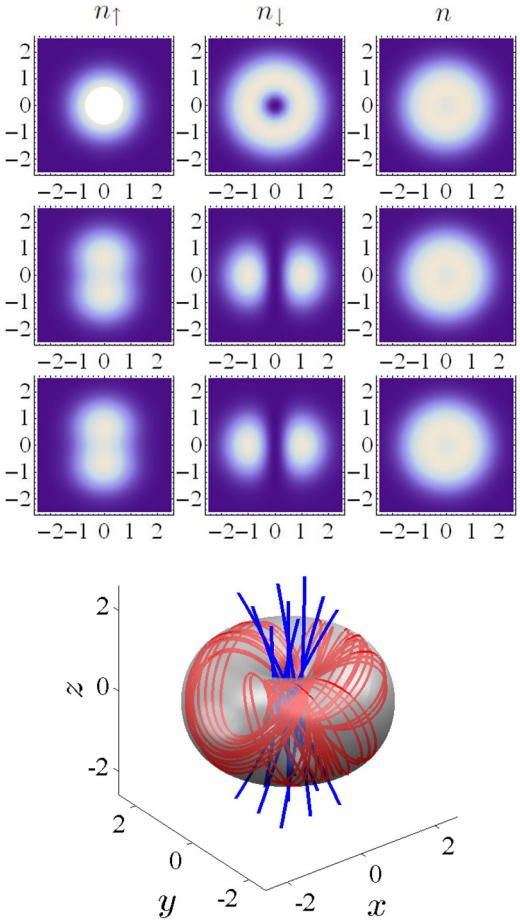

FIG. 2. (Color online) Density distribution and spin texture of phase I for $\alpha = -1.6$. All coordinates are in units of $l_T = \sqrt{\hbar/m\omega}$. Top: Three rows are densities in xy, yz, and xz planes, respectively; three columns are for up and down components and the total density as explicitly labeled above each column. Density distributions in xz and yz planes are the same due to the z-axis rotational symmetry. Bottom: 3D skyrmion spin texture $\mathbf{s}(\mathbf{r}) = \mathbf{S}(\mathbf{r})/n(\mathbf{r})$ of phase I. The streamline plot of $\mathbf{s}$ in a selected region is shown.

The density distributions and the spin texture of phases I and II are shown in Figs. 2 and 3, respectively. Typical features include the following.

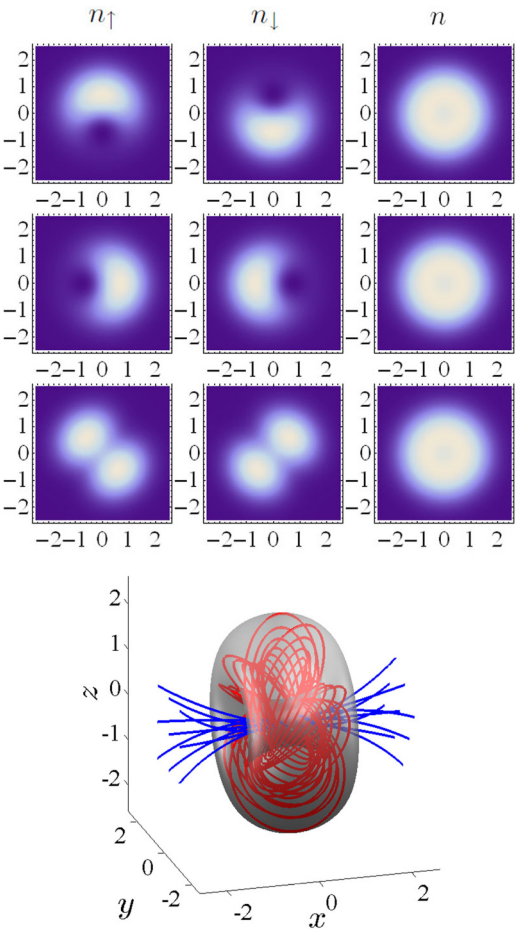

FIG. 3. (Color online) Density distribution and spin texture of phase II for $\alpha = -1.6$. All coordinates are in units of $l_T = \sqrt{\hbar/m\omega}$. Top: Three rows are densities in xy, yz, and xz planes, respectively; three columns are for up and down components and the total density as explicitly labeled above each column. Though the total density is isotropic again, the density distribution for the two components exhibits more complex symmetry as described in the text. Bottom: 3D skyrmion spin texture $\mathbf{s}(\mathbf{r}) = \mathbf{S}(\mathbf{r})/n(\mathbf{r})$ of phase II, which is roughly a $\pi/2$ rotation about the y axis of that in phase I. The topological structure of the spin texture is protected by the time-reversal symmetry.

A. Phase I

This phase contains two degenerate states $|c_+|^2 = 1$, $|c_-|^2 = 0$ and $|c_+|^2 = 0$, $|c_-|^2 = 1$. They are time-reversal states of each other and have similar density and spin texture except that the spin-up and spin-down components are exchanged. The order parameter for the former has the form

$$\Psi = (4\pi)^{-\frac{1}{2}} N_\alpha \begin{pmatrix} R_{00}(r) - i\alpha R_{01}(r)\cos\theta \\ -i\alpha R_{01}(r)\sin\theta e^{i\varphi} \end{pmatrix}.$$

The particle densities for the spin-up and spin-down components are

$$\begin{aligned} n_\uparrow &= (4\pi)^{-1} N_\alpha^2 \left(R_{00}^2(r) + \alpha^2 R_{01}^2(r)\cos^2\theta\right), \\ n_\downarrow &= (4\pi)^{-1} N_\alpha^2 \alpha^2 R_{01}^2(r)\sin^2\theta, \end{aligned} \tag{28}$$

which respect the rotational symmetry about the z axis and the parity symmetry, i.e., $n_{\uparrow,\downarrow}(\mathbf{r}) = n_{\uparrow,\downarrow}(r,\theta)$ and $n_{\uparrow,\downarrow}(r,\theta) = n_{\uparrow,\downarrow}(r,\pi-\theta)$. The densities of the two components in xz and yz planes are the same as shown in Fig. 2, which exhibit clearly characters of the p-wave state; i.e., the spin-up component is dumbbell-like while the spin-down component forms a torus. The total density on the other hand is isotropic—the sum of $n_\uparrow$ and $n_\downarrow$ in Eq. (28) relies only on the radius r.

This spin density calculated on the variational order parameter shows interesting spin texture described by

$$\begin{aligned} S_x &= (4\pi)^{-1} N_\alpha^2 \big(\alpha R_{00}(r) R_{01}(r)\sin\theta\sin\varphi \\ &\quad + \alpha^2 R_{01}^2(r)\sin\theta\cos\theta\cos\varphi\big), \\ S_y &= (4\pi)^{-1} N_\alpha^2 \big(-\alpha R_{00}(r) R_{01}(r)\sin\theta\cos\varphi \\ &\quad + \alpha^2 R_{01}^2(r)\sin\theta\cos\theta\sin\varphi\big), \\ S_z &= (8\pi)^{-1} N_\alpha^2 \big(R_{00}^2(r) + \alpha^2 R_{01}^2(r)\cos 2\theta\big). \end{aligned} \tag{29}$$

The average value of the spin in the xy plane is zero, i.e., $\langle S_x\rangle = \langle S_y\rangle = 0$. The spin texture $\mathbf{s}(\mathbf{r}) = \mathbf{S}(\mathbf{r})/n(\mathbf{r})$ is depicted in Fig. 2 and we find that spin density forms a torus near the xy plane and a bundle of nearly vertical streamlines of spin penetrate the central region of the torus. This skyrmionlike texture has been discussed in [20] and identified as the ground state in the $c < 1$ regime for an interaction parameter $c_0 = 100$. Li *et al.* [21] also found this ground-state skyrmion spin texture in the weak SO-coupling case for isotropic interaction $c = 1$. The term "skyrmionlike" means the absence of a boundary condition at $r \to \infty$ [20]; thus, the winding number for the texture is not an integer.

In order to get a deep understanding of the skyrmion nature of this ground state, we notice that the order parameter can be obtained from a local spin rotation from the polarized spinor wave function $\boldsymbol{\zeta}_z = (c_+, c_-)^T = (1,0)^T$,

$$\Psi_z = \exp(-i\Omega(\mathbf{r})\cdot\mathbf{s})\sqrt{n(\mathbf{r})}\boldsymbol{\zeta}_z, \tag{30}$$

supposing that $n(\mathbf{r}) = (4\pi)^{-1} N_\alpha^2 [R_{00}^2(r) + \alpha^2 R_{01}^2(r)]$ and $\boldsymbol{\Omega}(\mathbf{r}) = \omega(r)\mathbf{r}/r$. This operation rotates the spin at position $\mathbf{r}$ by an angle $\omega(r)$ about the axis $\mathbf{r}/r$. The rotation angle is position dependent; i.e., $\omega(r) = 2\arctan[\alpha R_{01}(r)/R_{00}(r)]$ and $\mathbf{s}$ is the usual spin angular momentum operators for spin-1/2. It is the explicit form of $\boldsymbol{\Omega}(\mathbf{r})$ that determines the specific texture of the skyrmion [27]. The polarized spinor order parameter $\boldsymbol{\zeta}_z$ has all spins being oriented in the positive z direction. After the rotation the order parameter Ψ_z for this skyrmion state is position dependent. The order parameter is the most symmetrically shaped skyrmion with the symmetric axis unrotated, which is identical with that already discussed in [27–32]. In those papers the 3D skyrmion states are proposed as excited states in pseudo-spin-1/2 or ferromagnetic spin-1 [27] Bose gases although they may be metastable.

B. Phase II

This phase again contains two degenerate states with $c_+ = c_- = \pm\frac{1}{\sqrt{2}}$ and $c_+ = -c_- = \pm\frac{1}{\sqrt{2}}$, which are time-reversal states of each other. They share similar density distribution and spin texture just like the case of phase I. The order parameter

for $c_+ = c_-$ has the form

$$\Psi = (8\pi)^{-\frac{1}{2}} N_\alpha \begin{pmatrix} R_{00}(r) - i\alpha R_{01}(r)(\cos\theta + \sin\theta e^{-i\varphi}) \\ R_{00}(r) - i\alpha R_{01}(r)(-\cos\theta + \sin\theta e^{i\varphi}) \end{pmatrix}, \tag{31}$$

and the particle densities for the two components are

$$\begin{aligned} n_\uparrow &= (8\pi)^{-1} N_\alpha^2 \big(R_{00}^2(r) + \alpha^2 R_{01}^2(r) \\ &\quad - 2\alpha R_{00} R_{01} \sin\theta \sin\varphi + \alpha^2 R_{01}^2 \sin 2\theta \cos\varphi\big), \\ n_\downarrow &= (8\pi)^{-1} N_\alpha^2 \big(R_{00}^2(r) + \alpha^2 R_{01}^2(r) \\ &\quad + 2\alpha R_{00} R_{01} \sin\theta \sin\varphi - \alpha^2 R_{01}^2 \sin 2\theta \cos\varphi\big). \end{aligned} \tag{32}$$

The density for each component consists of two parts: one is isotropic and common for both components as shown in the first and third lines in Eq. (32), while the second and fourth lines in Eq. (32), the other part for two components, are complementary to each other. This leads again to an isotropic total density. The overall density distribution of the two components can be visualized as two cashew nuts perpendicularly crossing and partially overlapping with each other. The distributions in xy, yz, and xz planes are shown in Fig. 3. The density distributions have symmetries when, e.g., the densities of two components are invariant under the combined operation of time reversal and π rotation about the x(or z) axis, i.e., $n_\uparrow(r,\pi-\theta,2\pi-\phi) = n_\downarrow(r,\theta,\phi)$ and $n_\uparrow(r,\theta,\pi+\phi) = n_\downarrow(r,\theta,\phi)$, while the π rotation about the y axis itself leaves the density distributions unchanged, i.e., $n_{\uparrow,\downarrow}(r,\pi-\theta,\pi-\phi) = n_{\uparrow,\downarrow}(r,\theta,\phi)$.

The spin texture associated with the order parameter is expressed as

$$\begin{aligned} S_x &= (8\pi)^{-1} N_\alpha^2 \big[R_{00}^2 + \alpha^2 R_{01}^2(\sin^2\theta\cos 2\varphi - \cos^2\theta)\big], \\ S_y &= (8\pi)^{-1} N_\alpha^2 \big(2\alpha R_{00} R_{01} \cos\theta + \alpha^2 R_{01}^2 \sin^2\theta \sin 2\varphi\big), \\ S_z &= (8\pi)^{-1} N_\alpha^2 \big(-2\alpha R_{00} R_{01} \sin\theta \sin\varphi \\ &\quad + \alpha^2 R_{01}^2 \sin 2\theta \cos\varphi\big). \end{aligned} \tag{33}$$

The average spin polarization along the z axis is zero, i.e., $\langle S_z\rangle = 0$. The spin texture $\mathbf{S}(\mathbf{r})/n(\mathbf{r})$ is presented in Fig. 3. The spin density in this case forms a torus near the yz plane and the fountainlike streamlines of spin pass through the hole of the torus, which is more or less like a $\pi/2$ rotation of the torus in phase I about the y axis. Similarly, this ground state can be obtained from a local spin rotation from the spinor order parameter $\boldsymbol{\zeta}_x = (c_+,c_-)^T = \frac{1}{\sqrt{2}}(1,1)^T$ that describes a system with all spins pointing to the positive x direction, i.e.,

$$\Psi_x = \exp(-i\boldsymbol{\Omega}(\mathbf{r})\cdot\mathbf{s})\sqrt{n(\mathbf{r})}\boldsymbol{\zeta}_x. \tag{34}$$

The spinor wave function $\boldsymbol{\zeta}_x$ is related to $\boldsymbol{\zeta}_z$ by a $\pi/2$ rotation around y. Owing to the non-Abelian nature of SO(3) rotation, the spin texture of phase II is different from the $\pi/2$ rotation around y of phase I. The difference between these two textures lies in the fact that the spin in the torus of phase I revolves the z axis following elliptical (oval) orbits that rotate gradually like the perihelion precession in celestial mechanics, while in phase II the orbits are closed loops. Apart from this, they indeed share the same topology determined by the same Ω as can be seen from the spin streamline plot in Fig. 3, because the topological spin texture is protected by time-reversal symmetry of the system. This skyrmion spin texture is proposed as the ground state in the regime of $c > 1$ in [20].

For a two-component Bose gas without SO coupling, it is known that the interaction parameter $c = 1$ represents the miscible to immiscible phase transition; i.e., the ground state is phase separated for $c > 1$, whereas for $c < 1$ the two components are coexisting which results in $S_z = 0$ to reduce the spin-dependent interaction. This important statement is valid even in the case of homogeneous Rashba spin-orbit-coupled Bose gases [8], in which $c = 1$ divides the miscible plane-wave phase and the immiscible stripe phase. However, this scenario fails for a trapped system due to the angular symmetry of the single-particle eigenstates. For Bose gas trapped in a harmonic trap, the spin-orbit coupling inevitably induces the mixing of different eigenstates [10,11], e.g., s and p spatial modes in a 3D harmonic oscillator. When the p-wave spatial mode is mixed in the wave function, the corresponding state always tends to be phase separated. To what extent is the state phase separated is determined by the weight of the p-wave state. We found that our ground state tends to be phase separated for both $c > 1$ and $c < 1$ regimes, but it is true that a larger coexisting region appears for weaker SO-coupling strength.

We find in this study that in both phase I and phase II the densities of the two components are spatially separated in three dimensions. We thus come up with a conclusion that phase separation of the spin components generally exists in 1D [33], 2D [10,11] and 3D SO-coupled boson gases. In our case it is the SO-coupling-induced p-wave spatial mode involved in the variational order parameter that drives the two spin components spatially separated. Previously, the skyrmions appearing in the two-component Bose gases without the SO coupling were all *excited* states, so the topologically stable skyrmions may be energetically unstable and additional stability mechanics are needed to stabilize them in the excited states. In the paper of Battye *et al.* [34], a stability mechanics was proposed for the non-spin-orbit-coupled model; the essential condition is phase separation. Our numerical results show that the spin-orbit-coupling energy participates in the mechanism here in the sense that stronger SO coupling tends to separate the two components even more distinctly, which obviously helps to stabilize the skyrmions. In this regard, our skyrmion ground states and related phase separation are consistent with those of [34]. Moreover, the stability of the ground-state skyrmions has been numerically checked in [20] for their parameters $c_0 = 100$, $0 < c_1/c_0 \lesssim 1$ ($c < 1$ in our case), and $c_1/c_0 < 0$ ($c > 1$), respectively. On the other hand, the topology of the skyrmion texture is protected by the time-reversal symmetry of the system; even the phase transition drastically changes the density structure.

V. SUMMARY

We have investigated variationally the ground-state phase diagram of weakly 3D spin-orbital-coupled two-component Bose gases in a harmonic trap. Two phases for the ground state are identified depending on intraspecies and interspecies interaction strength, and the corresponding density distribution and the spin texture are illustrated for optimized variational

parameters. Phase I is featured with the parity symmetric and rotational symmetric density distribution of both spin-up and spin-down components and skyrmion spin texture with torus in the xy plane and spin streamline passing through the central region, while phase II is characterized with density distribution possessing discrete π rotational symmetry about the y axis and π rotational time-reversal symmetry about x and z axes and the similar spin torus is in the yz plane, roughly a $\pi/2$ rotation of that in phase I about the y axis. In both phases, the density of two components is essentially phase separated. With increasing interaction strength, interesting phase transition occurs between the two phases, while the topology of ground-state spin textures is protected.

ACKNOWLEDGMENTS

This work is supported by NSFC under Grants No. 11234008 and No. 11474189, the National Basic Research Program of China (973 Program) under Grant No. 2011CB921601, and the Program for Changjiang Scholars and Innovative Research Team in University under Grant No. IRT13076.

[1] Y.-J. Lin, K. Jimenez-Garcia, and I. Spielman, Nature (London) **471**, 83 (2011).
[2] V. Galitski and I. B. Spielman, Nature (London) **494**, 49 (2013).
[3] T.-L. Ho and S. Zhang, Phys. Rev. Lett. **107**, 150403 (2011).
[4] Y. Li, L. P. Pitaevskii, and S. Stringari, Phys. Rev. Lett. **108**, 225301 (2012).
[5] W. Zheng, Z.-Q. Yu, X. Cui, and H. Zhai, J. Phys. B **46**, 134007 (2013).
[6] Z. Chen and H. Zhai, Phys. Rev. A **86**, 041604 (2012).
[7] H. Zhai, Rep. Prog. Phys. **78**, 026001 (2015).
[8] C. Wang, C. Gao, C.-M. Jian, and H. Zhai, Phys. Rev. Lett. **105**, 160403 (2010).
[9] C. J. Wu, M. S. Ian, and X. F. Zhou, Chin. Phys. Lett. **28**, 097102 (2011).
[10] H. Hu, B. Ramachandhran, H. Pu, and X.-J. Liu, Phys. Rev. Lett. **108**, 010402 (2012).
[11] B. Ramachandhran, B. Opanchuk, X.-J. Liu, H. Pu, P. D. Drummond, and H. Hu, Phys. Rev. A **85**, 023606 (2012).
[12] Y. Zhang, L. Mao, and C. Zhang, Phys. Rev. Lett. **108**, 035302 (2012).
[13] Z.-Q. Yu, Phys. Rev. A **87**, 051606 (2013).
[14] H. Zhai, Int. J. Mod. Phys. B **26**, 1230001 (2012).
[15] X. Cui and Q. Zhou, Phys. Rev. A **87**, 031604 (2013).
[16] Q. Zhou and X. Cui, Phys. Rev. Lett. **110**, 140407 (2013).
[17] D. L. Campbell, G. Juzeliūnas, and I. B. Spielman, Phys. Rev. A **84**, 025602 (2011).
[18] B. M. Anderson, G. Juzeliūnas, V. M. Galitski, and I. B. Spielman, Phys. Rev. Lett. **108**, 235301 (2012).
[19] B. M. Anderson, I. B. Spielman, and G. Juzeliūnas, Phys. Rev. Lett. **111**, 125301 (2013).
[20] T. Kawakami, T. Mizushima, M. Nitta, and K. Machida, Phys. Rev. Lett. **109**, 015301 (2012).
[21] Y. Li, X. Zhou, and C. Wu, arXiv:1205.2162.
[22] B. M. Anderson and C. W. Clark, J. Phys. B **46**, 134003 (2013).
[23] X.-F. Zhou, Y. Li, Z. Cai, and C.-J. Wu, J. Phys. B **46**, 134001 (2013).
[24] D.-W. Zhang, J.-P. Chen, C.-J. Shan, Z. D. Wang, and S.-L. Zhu, Phys. Rev. A **88**, 013612 (2013).
[25] T.-L. Ho and V. B. Shenoy, Phys. Rev. Lett. **77**, 3276 (1996).
[26] D. Varshalovich, A. Moskalev, and V. Khersonskii, *Quantum Theory of Angular Momentum* (World Scientific, Singapore, 1988).
[27] U. A. Khawaja and H. T. C. Stoof, Phys. Rev. A **64**, 043612 (2001).
[28] U. A. Khawaja and H. T. C. Stoof, Nature (London) **411**, 918 (2001).
[29] J. Ruostekoski and J. R. Anglin, Phys. Rev. Lett. **86**, 3934 (2001).
[30] C. M. Savage and J. Ruostekoski, Phys. Rev. Lett. **91**, 010403 (2003).
[31] I. F. Herbut and M. Oshikawa, Phys. Rev. Lett. **97**, 080403 (2006).
[32] A. Tokuno, Y. Mitamura, M. Oshikawa, and I. F. Herbut, Phys. Rev. A **79**, 053626 (2009).
[33] S. Gautam and S. K. Adhikari, Phys. Rev. A **90**, 043619 (2014).
[34] R. A. Battye, N. R. Cooper, and P. M. Sutcliffe, Phys. Rev. Lett. **88**, 080401 (2002).